

# Uranium ferromagnet with negligible magnetocrystalline anisotropy - $\text{U}_4\text{Ru}_7\text{Ge}_6$

Michal Vališka,<sup>1,\*</sup> Martin Diviš,<sup>1</sup> and Vladimír Sechovský<sup>1</sup>

<sup>1</sup>*Faculty of Mathematics and Physics, Charles University,  
DCMP, Ke Karlovu 5, CZ-12116 Praha 2, Czech Republic*

Strong magnetocrystalline anisotropy is a well-known property of uranium compounds. The almost isotropic ferromagnetism in  $\text{U}_4\text{Ru}_7\text{Ge}_6$  reported in this paper represents a striking exception. We present results of magnetization, AC susceptibility, thermal expansion, specific heat and electrical resistivity measurements performed on a  $\text{U}_4\text{Ru}_7\text{Ge}_6$  single crystal at various temperatures and magnetic fields and discuss them in conjunction with results of first-principles electronic-structure calculations.  $\text{U}_4\text{Ru}_7\text{Ge}_6$  behaves as an itinerant  $5f$ -electron ferromagnet ( $T_C = 10.7\text{ K}$ ,  $\mu_S = 0.85\ \mu_B/\text{f.u.}$  at  $1.9\text{ K}$ ). The ground-state easy-magnetization direction is along the  $[111]$  axis of the cubic lattice. The anisotropy field  $\mu_0 H_a$  along the  $[001]$  direction is only of  $\sim 0.3\text{ T}$ , which is at least 3 orders of magnitude smaller value than in other U ferromagnets. At  $T_r = 5.9\text{ K}$  the easy magnetization direction changes for  $[001]$  which holds at temperatures up to  $T_C$ . This transition causing a change of magnetic symmetry is significantly projected in low-field magnetization, AC susceptibility and thermal-expansion data whereas only a weak anomaly is observed at  $T_r$  in the temperature dependence of specific heat and electrical resistivity, respectively. The magnetoelastic interaction induces a rhombohedral (tetragonal) distortion of the paramagnetic cubic crystal lattice in case of the  $[111]$  ( $[001]$ ) easy-magnetization direction. The rhombohedral distortion is connected with two crystallographically inequivalent U sites. The ab initio calculated ground-state magnetic moment of  $1.01\ \mu_B/\text{f.u.}$  is oriented along  $[111]$ . The two crystallographically inequivalent U sites are a consequence of spin-orbit coupling of the U  $5f$ -electrons. In the excited state which is only  $0.9\text{ meV}$  above the ground state the moment points to the  $[001]$  direction in agreement with experiment. A scenario of the origin of the very weak magnetic anisotropy of  $\text{U}_4\text{Ru}_7\text{Ge}_6$  is discussed considering interactions of the U-ion  $5f$ -electron orbitals with the nearest neighbor ions.

PACS numbers: 75.30.Gw, 75.50.Cc, 75.40.Cx, 71.15.Mb

Keywords: Itinerant  $5f$ -electron ferromagnetism, low anisotropy, magnetostriction

## I. INTRODUCTION

Magnetocrystalline anisotropy (MA) is manifested by locking the magnetic moments in a specific orientation (usually the easy magnetization direction) with respect to crystal axes. A quantitative measure of MA, the anisotropy field  $H_a$ , is the magnetic field needed to be applied in the hard magnetization direction for reaching the easy-axis magnetization value. The key prerequisites of MA are the orbital moment of a magnetic ion, the spin-orbit (s-o) interaction coupling the orbital and spin moment, and interactions with neighboring ions<sup>1,2</sup>. The s-o interaction is a relativistic effect which becomes stronger in heavier atoms. Consequently MA dominates magnetism in materials with lanthanide and actinide ions bearing magnetic moments of the  $4f$ - and  $5f$ -electrons, respectively.

The widely accepted scenario of the origin of magnetocrystalline anisotropy involves the crystal electric field (CEF) interaction, the single-ion mechanism born in the electrostatic interaction of the anisotropic crystalline electric field (the potential created at the magnetic ion site by the electric charge distribution in rest of the crystal) with the aspherical charge cloud of the magnetic electrons. The electron orbital adopts the direction that minimizes the CEF interaction energy. The single-ion anisotropy is most often encountered in compounds with lanthanides having the well-localized  $4f$ -electrons<sup>3,4</sup>.

Contrary to the  $4f$ -orbitals deeply buried in the core

electron density of lanthanide ions the spatially extended uranium  $5f$ -electron wave functions interact with the overlapping  $5f$ -orbitals of the nearest neighbor U ions ( $5f$ - $5f$  overlap) and with valence electron orbitals of ligands ( $5f$ -ligand hybridization<sup>5</sup>). Consequently the  $5f$ -electron wave functions lose the atomic character and simultaneously the U magnetic moments melt down. Despite that the strong spin-orbit coupling induces a predominant orbital magnetic moment antiparallel to the spin moment in the spin-polarized  $5f$ -electron energy bands. This effect was first demonstrated for the itinerant  $5f$ -electron magnetism in UN<sup>6</sup>. In some cases very small or eventually zero total magnetic moment of a U ion are observed as a result of mutual compensation of the antiparallel spin and orbital component, respectively. The itinerant  $5f$ -electron ferromagnet  $\text{UNi}_2$ <sup>7</sup> with the U magnetic moment of few hundredths  $\mu_B$  serves as an excellent example as documented by results of polarized neutron measurements<sup>8</sup> and first principles electronic structure calculations<sup>9</sup>. Despite the itinerant character of magnetism  $\text{UNi}_2$  exhibits very strong magnetocrystalline anisotropy with  $\mu_0 H_a \gg 35\text{ T}$  at  $4.2\text{ K}$ <sup>10</sup>.

The very strong MA seems to be inherent to the uranium magnetism. The typical values of the MA field of most uranium intermetallic compounds are of the order of hundreds T<sup>11</sup>. The strong anisotropy is reported also for the cubic U pnictides and chalcogenides<sup>12,13</sup>.

The strong interaction of the spatially extended U  $5f$  orbitals with surrounding ligands in the crystal and

participation of  $5f$  electrons in bonding<sup>14,15</sup> imply an essentially different mechanism of magnetocrystalline anisotropy based on a two ion (U-U) interaction. The anisotropy of the bonding and  $5f$ -ligand hybridization assisted by the strong spin-orbit interaction are the key ingredients of the two-ion anisotropy in  $5f$ -electron magnets.

The systematic occurrence of particular types of anisotropy related to the layout of the U ions in a crystal lattice suggests that in materials, in which the U-U co-ordination is clearly defined in the crystal structure, the easy-magnetization direction is perpendicular to the nearest U-U links<sup>11,16</sup>. Cooper and co-workers<sup>17,18</sup> have formulated a relatively simple model of the two-ion interaction. This model, leading to qualitatively realistic results, is based on Coqblin-Schrieffer approach to the mixing of ionic  $f$ -states and conduction-electron states, in which the mixing term of the Hamiltonian of Anderson type is treated as a perturbation, and the hybridization interaction is replaced by an effective  $f$ -electron-band electron resonant exchange scattering. The theory has been further extended so that each partially delocalized  $f$ -electron ion is coupled by the hybridization to the band electron sea; and these both lead to a hybridization-mediated anisotropic two-ion interaction giving an anisotropic magnetic ordering.

In this paper we focus on magnetism in the  $\text{U}_4\text{Ru}_7\text{Ge}_6$  compound. Although the first  $\text{U}_4\text{Ru}_7\text{Ge}_6$  single crystals were grown already in late Eighties only a vague report on ferromagnetism ( $T_C \sim 7\text{ K}$ ,  $0.2\mu_B/\text{U}$  ion in  $5\text{ T}$  at  $4.3\text{ K}$ )<sup>19</sup> and no information on anisotropy can be found in literature. Therefore we have grown a high quality single crystal of this compound and measured on it the magnetization, AC susceptibility, thermal expansion, specific heat and electrical resistivity with respect to temperature and magnetic field. A weakly anisotropic ferromagnetism has been observed below  $T_C = 10.7\text{ K}$ . The ferromagnetic ground state is characterized by the easy-magnetization axis along the  $[111]$  crystallographic direction. A magnetic phase transition at which the easy magnetization axis changes from  $[111]$  to  $[001]$  is observed at  $T_r = 5.9\text{ K}$ . The  $[111]$  ( $[001]$ ) phase is associated with a tiny rhombohedral (tetragonal) distortion of the paramagnetic cubic crystal structure which hardly can be observed by the X-ray diffraction but we demonstrate that it can be indicated by thermal-expansion data. To shed more light on microscopic mechanisms responsible for the  $\text{U}_4\text{Ru}_7\text{Ge}_6$  magnetism in some aspects very unusual for U compounds we also performed first-principles electronic structure calculations.

## II. EXPERIMENTAL DETAILS

The  $\text{U}_4\text{Ru}_7\text{Ge}_6$  single crystal has been grown by Czochralski method in a tri-arc furnace from constituent elements (purity of Ru 3N5 and Ge 6N). The uranium metal was purified using Solid State Electrotransport

technique (SSE). Half of the crystal was wrapped in the Ta foil (purity 4N), sealed in a quartz tube under the vacuum of  $1 \cdot 10^{-6}\text{ mbar}$  and subsequently annealed at  $1000^\circ\text{C}$  for 7 days. The high quality of both crystals was verified by Laue diffraction using a Photonic Science X-Ray Laue system with a CCD camera and single crystal X-ray diffraction on a Rigaku R-Axis Rapid II diffractometer with a Mo lamp. A part of each, the as-cast and annealed single crystal, respectively, was pulverized and characterized by X-ray powder diffraction (XRPD) at room temperature on a Bruker D8 Advance diffractometer with a Cu lamp. The obtained data were evaluated by Rietveld technique<sup>20</sup> using FULLPROF/WINPLOTR software<sup>21,22</sup>. The chemical composition of each single crystal was verified by a scanning electron microscope (SEM) Tescan Mira I LMH equipped with an energy dispersive X-ray (EDX) detector Bruker AXS. Samples for individual experiments were afterward cut from the annealed crystal with a fine wire saw to prevent induction of additional stresses and lattice defects.

The magnetization (in a magnetic field up to 7 T applied along the  $[001]$  and  $[111]$  directions, respectively) and AC susceptibility (the AC magnetic field with the amplitude of  $300\mu\text{T}$  applied along  $[001]$ ) were measured by a SQUID magnetometer in MPMS 7T in the temperature range from 1.9 K to 300 K. The magnetization along  $[111]$  was measured up to 14 T by a VSM device at a PPMS 14T. Specific heat data were collected by the thermal relaxation technique in the temperature range from 0.4 to 20 K in the magnetic fields up to 9 T by a PPMS 9T. The electrical resistivity measurements were realized with the ACT option of the PPMS instruments with AC current applied along  $[100]$  and  $[111]$ , respectively, in the temperature range from 1.9 K to 300 K. The MPMS 7T and both the PPMS apparatuses are of Quantum Design Inc. production. The thermal expansion measurements along the  $[100]$ ,  $[001]$  and  $[111]$  directions, respectively, in the temperature range from 1.9 K to 30 K using a miniature capacitance dilatometer<sup>23</sup> implemented in the PPMS 9T. All the instrumentation mentioned above is a part of the Magnetism and Low Temperature Laboratories – MLTL (<http://mltl.eu/>).

## III. RESULTS

### A. Crystal structure and chemical composition

The Rietveld refinement of XRPD data collected on the pulverized as-cast (see the powder pattern in Figure 1) and annealed single crystal, respectively, confirmed previous reports<sup>19,24,25</sup> that  $\text{U}_4\text{Ru}_7\text{Ge}_6$  possesses at room temperature a cubic crystal structure of the  $Im\bar{3}m$  space group. The corresponding lattice parameters (see Table 1) determined for the as cast and annealed crystal, respectively, are nearly identical.

Elemental mapping by EDX confirmed homogeneity of all the studied samples. The average of multiple point

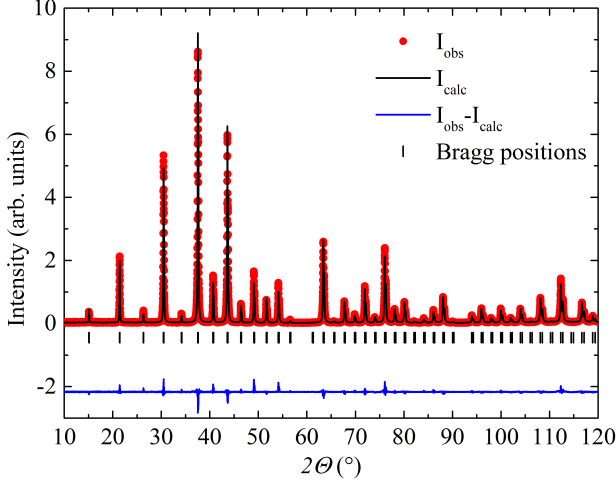


Figure 1. X-ray powder diffraction pattern of a pulverized  $\text{U}_4\text{Ru}_7\text{Ge}_6$  as cast single crystal.

Space group	$Im\bar{3}m$	as-cast	annealed
$a$		8.2934(2) Å	8.2933(3) Å
U( $x, y, z$ ), 8c	(0.25, 0.25, 0.25)	(0.25, 0.25, 0.25)	(0.25, 0.25, 0.25)
Ru <sub>1</sub> ( $x, y, z$ ), 12d	(0.25, 0, 0.5)	(0.25, 0, 0.5)	(0.25, 0, 0.5)
Ru <sub>2</sub> ( $x, y, z$ ), 2a	(0, 0, 0)	(0, 0, 0)	(0, 0, 0)
Ge( $x, y, z$ ), 12e	(0.31375(13), 0, 0)	(0.31360(11), 0, 0)	(0.31360(11), 0, 0)

Table I. Results of structure analysis.

scans from the different part of the sample gives resulting stoichiometry 4.4(4):6.9(2):5.7(1). It points to a slight Ge deficiency.

### B. Low temperature magnetization

The magnetization curves  $M(\mu_0 H)$  measured at 1.9 K in a magnetic field applied along the [001] and [111] direction, respectively, document that  $\text{U}_4\text{Ru}_7\text{Ge}_6$  is at this temperature ferromagnetic with the easy magnetization direction along the [111] axis (see Figure 2). The spontaneous magnetization  $M_{S[111]} = 0.88(1) \mu_B$  (obtained as an extrapolation of the  $M_{[111]}(\mu_0 H)$  dependence to  $\mu_0 H = 0$  T). The spontaneous magnetization value along the [001] direction is lower,  $M_{S[001]} = 0.51(1) \mu_B$ , respectively. This value is in very good agreement with Néel phase law<sup>26</sup> for a cubic system. It proposes that  $M_{S[001]}$  can be obtained from the  $M_{S[111]}$  value multiplied by the appropriate direction cosine – i.e.  $M_{S[001]} = \sqrt{\frac{1}{3}} M_{S[111]}$ . For fields higher than 0.3 T the  $M_{[111]}(\mu_0 H)$  and  $M_{[001]}(\mu_0 H)$  curves merge (we estimate the  $\mu_0 H_a$  value 300 mT), however, do not saturate in the field up to the 14 T where the magnetization reaches the value of  $1.4 \mu_B/\text{f.u.}$ . The poor saturation of the magnetization in high magnetic fields is typical for itinerant electron ferro-

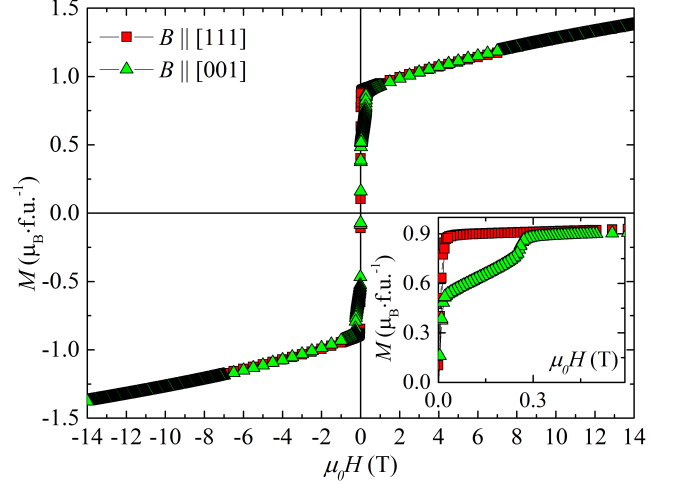


Figure 2. Field dependence of magnetization isotherms of  $\text{U}_4\text{Ru}_7\text{Ge}_6$  at 1.9 K for [111], and [001] directions of applied magnetic field. Inset shows a low field detail.

magnets. The increasing magnetic moment with increasing the magnetic field is then reflecting the magnetic-field induced change of electronic structure (additional splitting of the majority and minority subbands).

The observed very weak magnetization anisotropy makes  $\text{U}_4\text{Ru}_7\text{Ge}_6$  a unique exception among the U ferromagnets which are by rule strongly anisotropic with anisotropy fields of several hundred T<sup>11</sup>. In the next chapter we approach this issue by the first-principles electronic structure calculations focused on the microscopic origin of U magnetic moments and magnetocrystalline anisotropy.

### C. First-principles calculations

To obtain microscopic information about magnetism in  $\text{U}_4\text{Ru}_7\text{Ge}_6$  we applied the first-principles methods based on the density functional theory (DFT). The Kohn-Sham-Dirac 4-components equations have been solved by using the latest version of the full-potential-local-orbitals (FPLO) computer code<sup>27</sup>. Several  $k$ -meshes in the Brillouin zone were involved to ensure the convergence of charge densities, total energy and magnetic moments. For the sake of simplicity we assumed a collinear ferromagnetic structure. In  $\text{U}_4\text{Ru}_7\text{Ge}_6$  the total ground-state magnetic moment has been found pointing along the [111] direction. Due to the s-o interaction the symmetry is reduced from 48 to 12 symmetry operations. Instead of four symmetrically equivalent U ion sites in the scalar relativistic treatment with a spin-only magnetic moment we have the spin and orbital angular momenta coupled by the relativistic s-o interaction which divides the U ions in two subgroups consistently with the expected rhombohedral distortion induced by magnetoelastic interaction in case of the [111] easy magnetization direction. The U ions

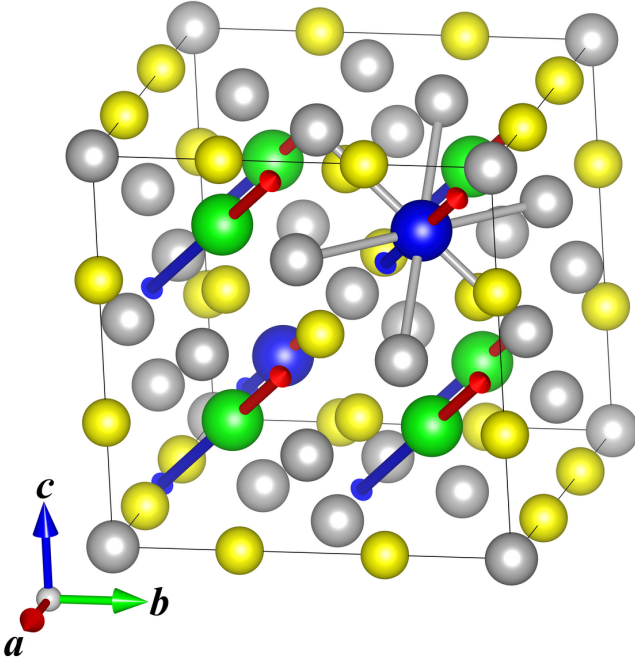


Figure 3. Structure of  $\text{U}_4\text{Ru}_7\text{Ge}_6$  together with magnetic moments from theoretical calculations. Arrows for magnetic moments are in proper relative scale but in arbitrary units.  $\text{U}_1$  ions are blue,  $\text{U}_2$  are green,  $\text{Ru}_3$  and  $\text{Ru}_4$  are gray and  $\text{Ge}_5$  are yellow.

in the first subgroup at the  $\text{U}_1$  positions (0.25, 0.25, 0.25) and (0.75, 0.75, 0.75), respectively have a very small total magnetic moment of  $0.01 \mu_B$  due to cancellation of the almost equal-size antiparallel spin and orbital moment (see Figure 3). The second subgroup includes the U ions at the remaining six  $\text{U}_2$  positions bearing the spin magnetic moment of  $-0.56 \mu_B$  and the orbital magnetic moment of  $0.79 \mu_B$ . There are also some hybridization-induced Ru magnetic moments, which summed up give  $0.29 \mu_B$ , whereas the calculated Ge magnetic moment is negligible. The summation over the seventeen ions (one formula unit) in the primitive crystallographic cell gives the total magnetic moment of  $1.01 \mu_B$  which is somewhat larger than the spontaneous magnetic moment determined by experiment.

We have also performed relativistic calculation with the moment along [001]. In this case the cubic symmetry is reduced to tetragonal and all U moments have the same value of spin ( $-0.529 \mu_B$ ) and orbital ( $0.706 \mu_B$ ) component.

When calculating the magnetocrystalline anisotropy energy between the configurations of magnetic moments aligned along the [111] and [001] axis the values of the total energy were used. In agreement with experiment we have found the ground state with the total moment pointing to the [111] direction. The excited state with the moment pointing to the [001] direction is 0.9 meV above the ground state. This value is as to order of mag-

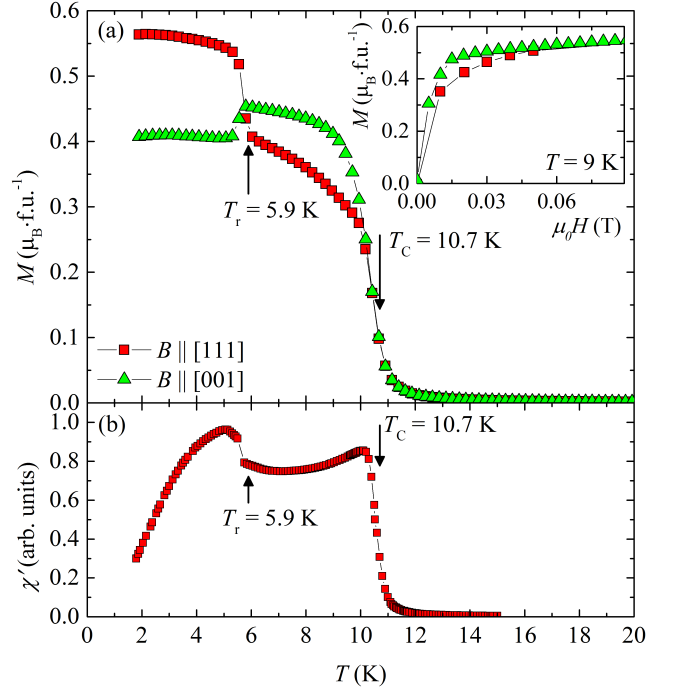


Figure 4. Temperature dependence of the magnetization of  $\text{U}_4\text{Ru}_7\text{Ge}_6$  measured in the magnetic field of 10 mT (in the ZFC regime) applied along the [111] and [100] direction, respectively (a) and temperature dependence of the AC susceptibility in the AC field applied along the [111] (b). Inset in the upper panel shows field dependence of magnetization at 9 K.

nitude in agreement with the energy corresponding to  $T_r$ , the temperature of [111] to [100] spin reorientation transition.

#### D. Magnetization near the phase transitions

The Curie temperature,  $T_C$ , of a ferromagnet is frequently estimated as the temperature of the inflection point of the  $M$  vs.  $T$  curve measured in a low magnetic field and/or of the temperature dependence of the AC-susceptibility. In Figure 4 (a) one can see that the temperature dependences of magnetization  $M(T)$  measured in the external magnetic field of 10 mT applied along the [111] and [100] direction, respectively, have one inflection point at the same temperature of  $10.6 \pm 0.1$  K ( $\sim T_C$ ) and are crossing at  $T_r = 5.9 \pm 0.1$  K. Two sharp anomalies at corresponding temperatures can be seen in the  $\chi_{AC}(T)$  dependence seen in the Figure 4 (b). These results clearly document that  $\text{U}_4\text{Ru}_7\text{Ge}_6$  orders at  $T_C$  ferromagnetically with the easy magnetization axis [100] (which is demonstrated by the 9 K magnetization isotherms in the inset of Figure 4 (a)). At  $T_r$  it undergoes a spin reorientation transition to the ground state characterized by the easy magnetization axis along [111].

A rigorous way of determining Curie temperature of



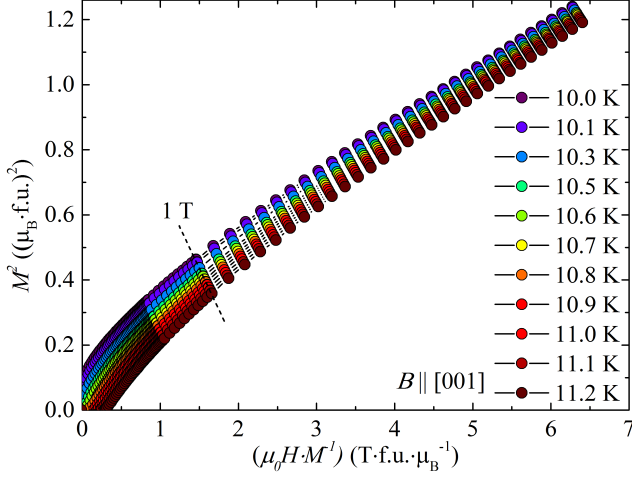


Figure 5. Arrott plots for  $\text{U}_4\text{Ru}_7\text{Ge}_6$  in the magnetic field applied along the [001] direction.

a ferromagnet from magnetization data is based on the analysis of Arrott plots ( $M^2$  vs.  $\mu_0 H/M$ )<sup>28</sup>. Linear Arrott plots are in fact a graphical representation of the Ginsburg-Landau mean field theory of magnetism in the vicinity of the ferromagnetic to paramagnetic second order phase transition. In Figure 5 one can see that the Arrott plots for  $\text{U}_4\text{Ru}_7\text{Ge}_6$  in the magnetic field applied along the easy magnetization direction [001] are almost linear with varying slope for magnetic fields between 1 and 7 T whereas for lower fields they became slightly concave. The linear extrapolations of high-field data to the vertical axis are marking the values of  $M^2$ , which are considered as estimates of the square spontaneous magnetization  $M_S^2$ . The spontaneous magnetization as the order parameter of a ferromagnetic phase vanishes at  $T_C$ . Note that the use of the linear extrapolations from high fields in case of the concave curvature of  $\text{U}_4\text{Ru}_7\text{Ge}_6$  Arrott plots in low fields leads to a certain overestimation of  $M_S$  values and consequently to a higher estimated  $T_C$  value.

A more precise  $T_C$  value may be expected from the generalized approach using the Arrott-Noakes equation of state  $(\mu_0 H/M)^{1/\gamma} = (T - T_C)/T_1 + (M/M_1)^{1/\beta}$ , where  $M_1$  and  $T_1$  are material constants<sup>29</sup>. We re-analyzed our data by plotting them as  $M^{1/\beta}$  vs.  $(\mu_0 H/M)^{1/\gamma}$  while  $\beta$  and  $\gamma$  values were chosen to get the best possible linearity of these plots keeping them parallel with constant slope. The values  $\beta = 0.31 \pm 0.03$  and  $\gamma = 0.81 \pm 0.04$  lead to a linear dependence in the broad field range except the very low fields. This construction is plotted in Figure 6 for all measured isotherms. This approach leads to  $T_C = 10.7 \pm 0.1$  K (see inset of Figure 6) that is in agreement with the estimated value from the low field magnetization data.

The critical exponent  $\delta$  in ideal case might satisfy the Widom scaling relation  $\delta = 1 + \gamma/\beta$  (Ref.<sup>30</sup>) which for  $\beta$  and  $\gamma$ , provided by the Arrott-Noakes analysis, gives  $\delta =$

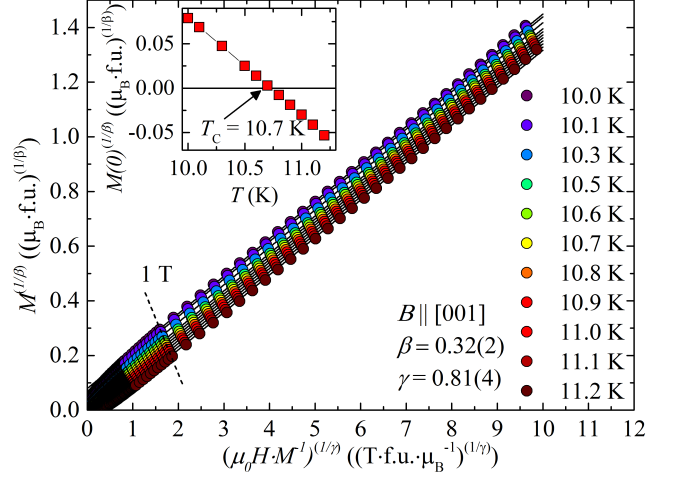


Figure 6. Arrott-Noakes plots reflecting the equation of states (with  $\beta = 0.31 \pm 0.03$  and  $\gamma = 0.81 \pm 0.04$ ) for  $\text{U}_4\text{Ru}_7\text{Ge}_6$  in the magnetic field applied along the [001] direction.

$B \parallel$	$\mu_{\text{eff}} (\mu_B/\text{U})$	$\theta_P (\text{K})$	$\chi_0 \cdot 10^{-8} (\text{m}^3 \cdot \text{mol}^{-1})$
[001]	1.43	7.5	5.8
[111]	1.43	8.1	5.7

Table II. Results of the modified Curie-Weiss fit in the temperature interval 30 – 300 K.

$3.52 \pm 0.04$  that is in excellent agreement with the value  $\delta = 3.55 \pm 0.04$  obtained from direct fitting of the critical isotherm that should follow  $M \sim (\mu_0 H)^{1/\delta}$ . Note that the critical exponents for the mean field approximation are  $\beta = 0.5$ ,  $\gamma = 1$  and  $\delta = 3$  (Ref.<sup>31</sup>), however, we should mention the work of Yamada<sup>32</sup> who has shown that the spin fluctuations in weak itinerant ferromagnets lead to the Arrott plots linear in strong magnetic fields and bent downwards at the region of small magnetizations.

### E. Paramagnetic susceptibility

The nearly identical temperature dependences of paramagnetic susceptibility measured along the [111] and [100] direction, respectively document isotropic paramagnetic state of  $\text{U}_4\text{Ru}_7\text{Ge}_6$  (see the  $1/\chi$  vs.  $T$  plot in Figure 7). The susceptibility values at temperatures above 30 K can be well fitted with a modified Curie-Weiss law in temperature range with parameters shown in Table II.

### F. Heat capacity

Heat capacity data show a clear anomaly at 10.7 K as displayed in Figure 8. This temperature coincides with the  $T_C$  value determined from magnetization data by

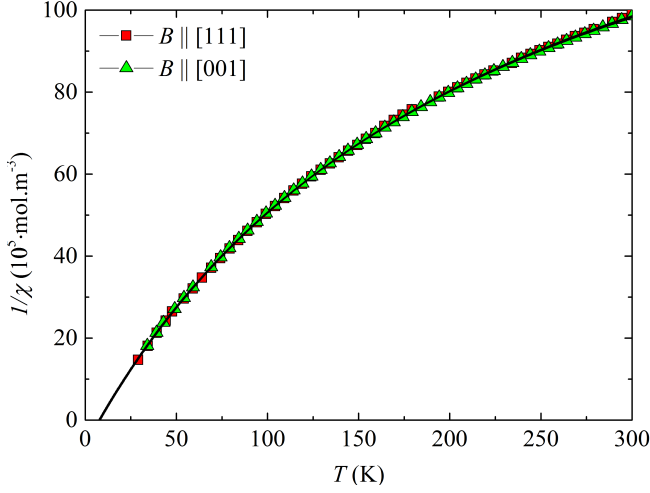


Figure 7. Temperature dependence of inverse susceptibility of  $\text{U}_4\text{Ru}_7\text{Ge}_6$  in the magnetic field of 1 T applied along the [111] and [001] direction. The full curve represents the fit with a modified Curie-Weiss law.

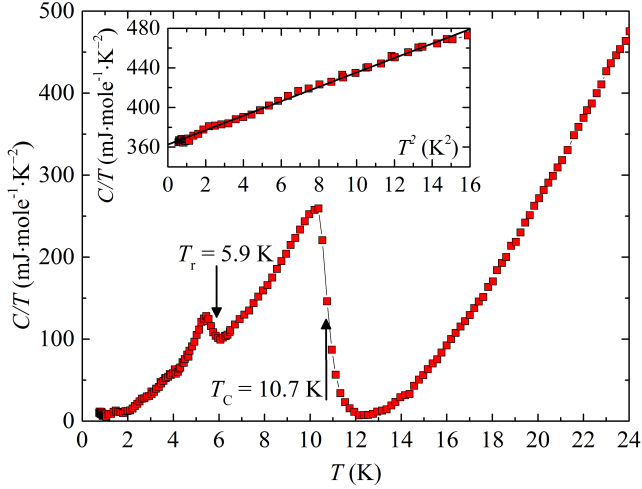


Figure 8. Temperature dependence of the heat capacity ( $C/T$  vs.  $T$  plot) of  $\text{U}_4\text{Ru}_7\text{Ge}_6$ . Inset: the  $C/T$  vs.  $T^2$  plot.

Arrott-Noakes plot analysis. The estimated magnetic entropy at  $T_C$  (i.e. integrated from 0.3 K to  $T_C$ ) of  $0.2 \cdot R \ln 2$  is much lower than  $R \ln 2$  which is another evidence of itinerant electron magnetism in  $\text{U}_4\text{Ru}_7\text{Ge}_6$ . The magnetic moment reorientation transition at  $T_r$  is reflected in a tiny but clear peak at this temperature.

The gamma coefficient of the electronic specific heat determined from a standard  $C/T$  vs.  $T^2$  plot (see Inset in Figure 8) constructed from data below 4 K amounts to  $362 \text{ mJ} \cdot \text{mol}^{-1} \cdot \text{K}^{-2}$ . The value related to one U ion =  $90.5 \text{ mJ} \cdot \text{mol}^{-1} \cdot \text{K}^{-2}$  reflects presence of the U  $5f$ -electron states at  $E_F$  similar to numerous other U intermetallics with itinerant  $5f$ -electrons which usually exhibit elevated values somewhere between 30 and  $100 \text{ mJ} \cdot \text{mol}^{-1} \cdot \text{K}^{-2}$  per U ion.

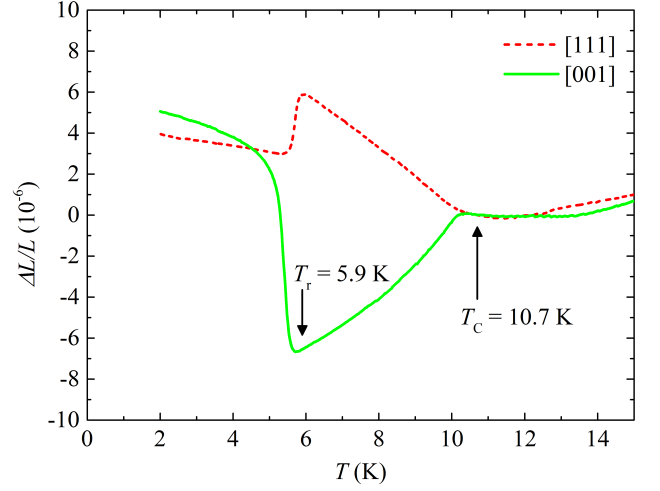


Figure 9. Linear thermal expansion of  $\text{U}_4\text{Ru}_7\text{Ge}_6$  along the [001] and [111] directions, respectively.

### G. Thermal expansion and magnetostriction

The linear thermal expansion  $\Delta L/L$  measured along the [001] ([111]) direction in zero magnetic field which can be seen in Figure 9, shows two distinct anomalies which can be attributed to the magnetic phase transitions revealed by magnetization measurements. When cooling from higher temperatures a downturn (upturn) having onset in the vicinity of  $T_C$  is followed by a steep increase (decrease) of the corresponding  $\Delta L/L$  below  $\sim 6$  K ( $\sim T_r$ ).

Most of the thermal expansion studies of ferromagnets revealing the spontaneous magnetostriction at temperatures  $T < T_C$  were done by using the X-ray or neutron diffraction<sup>33</sup>. We investigated the crystal structure of  $\text{U}_4\text{Ru}_7\text{Ge}_6$  by X-ray powder diffraction at low temperatures down to 3 K. No change of diffraction within the experimental error data has been observed below 11 K.

From Figure 9 it is however evident that our thermal expansion data obtained by dilatometer on the  $\text{U}_4\text{Ru}_7\text{Ge}_6$  single crystal clearly demonstrate the existence of lattice distortions in ferromagnetic state. The distortions here are, however, very small ( $< 10^{-5}$ ).

The dilatometer enables us to determine the crystal distortions along the 3 perpendicular crystal axes [100], [010] and [001], respectively. To study the corresponding linear spontaneous magnetostriction of a ferromagnet with a dilatometer one should perform measurements on a single crystal sample containing only one ferromagnetic domain. Knowing magnetization data we studied the phase with the easy magnetization along [001] stable at temperatures  $T_r < T < T_C$  in the following way. We first cooled the crystal down to 6.2 K (the temperature just above the onset of the spin reorientation transition) in the field of 1 T parallel to the [001] direction, at this temperature decreased the magnetic field down to 30 mT and then measured the thermal expansion in the

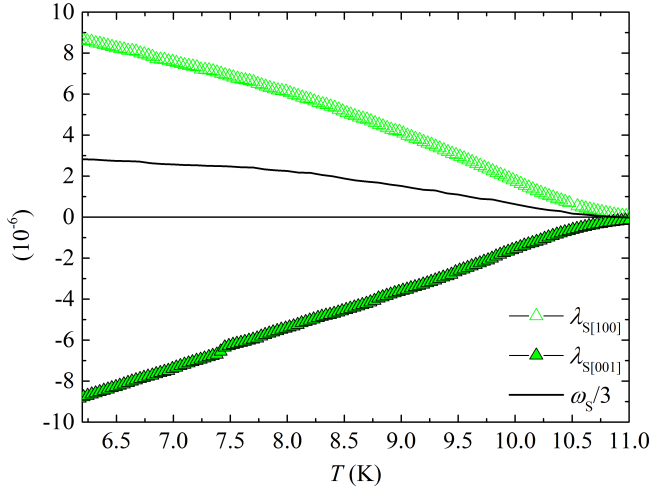


Figure 10. Linear thermal expansion of  $\text{U}_4\text{Ru}_7\text{Ge}_6$  along the [001] and [100] direction in the magnetic field of 30 mT applied along [001] and the corresponding thermal volume expansion at temperatures from 6.2 K to  $T_C$ . The presented data are considered as the best estimation of corresponding spontaneous magnetostriction (see text).

longitudinal  $(\Delta L/L)_{[001]}$  and transversal  $(\Delta L/L)_{[100]}$  geometry, respectively, with increasing temperature up to  $T_C$ . In this experiment the thermal expansion along the  $c$ - and  $a$ -axis, respectively, of the ferromagnetic tetragonally distorted structure was measured. The field of 30 mT applied along [001] is the minimum field maintaining the single-domain sample with the magnetic moment oriented along the  $c$ -axis. These  $(\Delta L/L)_{[001]}$  and  $(\Delta L/L)_{[100]}$  thermal expansion data can be taken as a reasonable approximation of spontaneous linear magnetostriction (denoted as  $\lambda_{S[001]}$  and  $\lambda_{S[100]}$ , respectively).

One can see that the values of the spontaneous tetragonal distortion is negative (the  $c$ -axis shrinks) and very small ( $\lambda_{S[001]} \sim -9 \cdot 10^{-6}$  at 6.2 K). Simultaneously the  $a$ -axis expands ( $\lambda_{S[100]} = \lambda_{S[010]} \sim 9 \cdot 10^{-6}$  at 6.2 K). Figure 10 shows also the corresponding spontaneous thermal volume expansion usually denoted as  $\omega_S (= 2 \cdot \lambda_{S[100]} + \lambda_{S[001]})$ . As expected for an itinerant electron ferromagnet the volume of the  $\text{U}_4\text{Ru}_7\text{Ge}_6$  lattice expands below  $T_C$ . Reasonable data can be collected only down to 6.2 K. Below this temperature the magnetic-moment-reorientation transition from [001] to [111] direction commences, the direction of magnetic moment becomes uncertain despite the magnetic field of 30 mT is applied along [001].

## H. Electrical resistivity

The almost identical corresponding values of the electrical resistivity measured for current along [111] and [100] direction, respectively, over the entire temperature range 2–300 K indicates a quite isotropic electron trans-

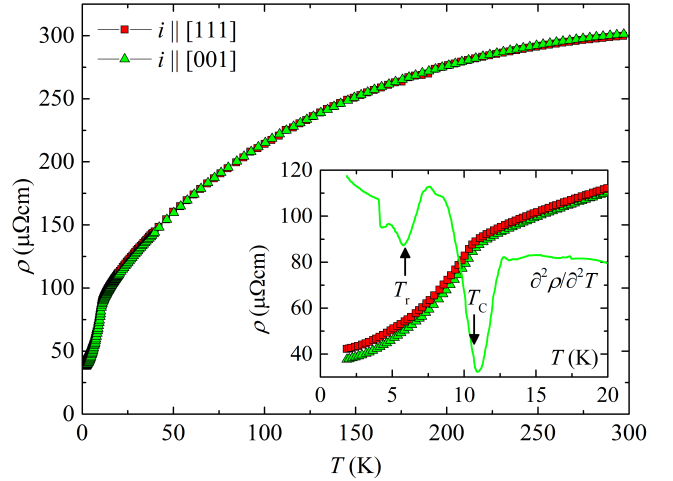


Figure 11. Temperature dependence of electrical resistivity of the  $\text{U}_4\text{Ru}_7\text{Ge}_6$  measured for current along [111] and [100] direction.

port in  $\text{U}_4\text{Ru}_7\text{Ge}_6$  (see Figure 11). The downward concave  $\rho(T)$  curve in the paramagnetic state resembles rather the behavior of transition metal compounds. This trend changes at  $T_C$  to the low-temperature upward concave curve with the  $T^2$  scaling. When inspecting the second derivative we observe a deep minimum of  $\partial^2 \rho / \partial T^2$  at  $T_C$  and a local minimum at  $T_r$ .

## IV. DISCUSSION

The  $M(\mu_0 H)$  curve measured for the hard magnetization direction [100] merges with the easy-magnetization direction [111] curve near 300 mT as seen in Figure 2. This anisotropy field of  $\text{U}_4\text{Ru}_7\text{Ge}_6$  is an unprecedentedly low value ever observed for a uranium intermetallic compound. Moreover, we observed an entirely isotropic paramagnetic susceptibility and electrical resistivity which up to our best knowledge has not been reported for any uranium  $5f$ -electron ferromagnet.

One may argue that the almost isotropic magnetism in  $\text{U}_4\text{Ru}_7\text{Ge}_6$  is a consequence of the itinerant character of U  $5f$ -electron magnetic moment. The spontaneous magnetic moment of this compound is  $\sim 0.85 \mu_B/\text{f.u.}$ , which provides an average moment of  $\sim 0.21 \mu_B/\text{U}$  ion when supposing negligible contributions from Ru and Ge ions. This value is 4 times larger than the U-born magnetic moment of the itinerant  $5f$  electron ferromagnet  $\text{UNi}_2$ <sup>7–10</sup> which, in contrary, exhibits huge magnetocrystalline anisotropy with the anisotropy field  $\gg 35 \text{ T}$ <sup>10</sup>.

Both our magnetization data and ab initio calculations clearly show that the easy magnetization direction of  $\text{U}_4\text{Ru}_7\text{Ge}_6$  in the ground state is [111]. As a result of magnetoelastic interaction<sup>34</sup>, the ferromagnetic ordering at temperatures below  $T_C$  is accompanied by the spontaneous magnetostriction causing a distortion of a crystal

lattice related to the easy-magnetization direction. These distortions are in ferromagnetic materials possessing cubic crystal structure in paramagnetic state (at temperatures  $T > T_C$ ) the spontaneous magnetostriction leads to a distortion lowering the paramagnetic cubic to tetragonal, orthorhombic and rhombohedral symmetry for the [001]-, [110]- and [111]-easy-magnetization direction, respectively. The expected rhombohedral distortion of the cubic  $U_4Ru_7Ge_6$  lattice in the ferromagnetic ground state is so tiny that it falls within the experimental error of a standard X-ray diffraction but is clearly indicated by thermal expansion results at low temperatures. As a consequence of the distortion the one equivalent crystallographic site common for all U ions in the cubic lattice splits into two inequivalent ones which is confirmed by ab initio calculations.

Our magnetization results also reveal that the easy-magnetization direction holds onto the [111] axis only at low temperatures up to  $T_r$  ( $= 5.9$  K) whereas at higher temperatures up to  $T_C$  the easy-magnetization direction is unambiguously along [001] and the paramagnetic cubic lattice is tetragonally distorted along this direction. This finding is in good agreement with the theoretical calculations which reveal the excited state with the [001] easy magnetization 0.9 meV above the ground state.

The magnetic moment reorientation transition in  $U_4Ru_7Ge_6$  at  $T_r$  is manifested in specific features (anomalies) which we observed in the temperature dependencies of magnetization (Figure 4a), AC susceptibility (Figure 4b), specific heat (Figure 8), thermal expansion (Figure 9) and electrical resistivity (Figure 11). It is in fact an order-to-order magnetic phase transition accompanied by structural distortion due to notable magnetoelastic coupling. These phase transitions are known to be of the first order type (e.g.  $HoAl_2$ <sup>35</sup>). The thermal expansion anomalies seen in Figure 9 at  $T_C$  and  $T_r$ , respectively, may be viewed as an illustrative examples of the second and first order type phase transitions. However, the first order phase transition is to be accompanied by latent heat which we were unable to detect by detailed specific-heat measurement and the  $T_r$  related specific-heat anomaly is considerably broader than expected for a first order phase transition. We attribute the lack of observables pointing to the presence of latent heat to the complex domain structure processes during the spin reorientation in the multidomain sample in the vicinity of  $T_r$  and our tentative determination has to be confirmed by a designed method allowing determination of order type by other means (e.g. phase coexistence in  $\mu$ SR).

The anisotropy field values in U ferromagnets are typically hundreds T whereas in  $U_4Ru_7Ge_6$  it is roughly 3 orders of magnitude smaller value. When inspecting crystal structures we observe that in all cases of the U ferromagnets characterized by high values of anisotropy field the U ions have some U nearest neighbors. Contrary, the individual U ions in  $U_4Ru_7Ge_6$  are buried inside the Ru and Ge polyhedra preventing direct connection to any nearest U ion which should have consequences for magnetism<sup>36</sup>.

The direct  $5f$ - $5f$  overlap of U electron orbitals is probably behind the huge magnetic anisotropy of U compounds. The symmetry of the network of U nearest neighbors determines the type of magnetic anisotropy in these materials<sup>11</sup>. The driving mechanism of magnetic anisotropy in  $U_4Ru_7Ge_6$  is presumably the hybridization of U  $5f$ -electron states with the  $4d$ -electron states of surrounding Ru ions which are in hexagonal arrangement, perpendicular to the easy magnetization direction [111].

Onset of itinerant electron ferromagnetism is usually accompanied by a positive spontaneous magnetovolume effect<sup>37,38</sup>. Also our thermal expansion data show this tendency despite the negative value of  $\lambda_{S[001]}$ . Unfortunately, the measurements using dilatometer cannot be extended to temperatures lower than  $T_r$  because the body diagonals representing the [111] easy magnetization direction are not perpendicular and therefore an experiment analogous to that for  $T_r < T < T_C$  is not accessible.

## V. CONCLUSIONS

We have demonstrated by experiment and by calculations the almost isotropic ferromagnetism in  $U_4Ru_7Ge_6$  which represents a case contrasting the huge magnetocrystalline anisotropy in so far reported ferromagnetic uranium compounds exhibiting by rule at least 3 orders of magnitude larger values of anisotropy field. The ground-state easy-magnetization direction is along the [111] axis of the cubic lattice as found both by experiment and by calculations. At  $T_r = 5.9$  K the easy magnetization direction changes for [100] which holds at temperatures up to  $T_C$  as found by experiments. This is in agreement with calculations revealing that the moment pointing to the [001] direction is characteristic for the excited state which is only 0.9 meV above the ground state. This spin reorientation transition is significantly projected in low-field magnetization, AC susceptibility and thermal-expansion data and causes also a weak anomaly at  $T_r$  visible in the temperature dependence of specific heat and electrical resistivity, respectively.

The magnetoelastic interaction induces a rhombohedral (tetragonal) distortion of the paramagnetic cubic crystal lattice in case of the [111]([001]) easy-magnetization direction. The rhombohedral distortion leads to emergence of two crystallographically inequivalent U sites which is also in agreement with results of calculations. We propose a scenario of the very weak magnetic anisotropy of  $U_4Ru_7Ge_6$  connected with the lack of direct  $5f$ - $5f$  overlaps of orbitals of nearest U – U neighbors. These are prevented by the specific crystal structure in which the individual U ions are trapped inside of the Ru, Ge polyhedra.



## ACKNOWLEDGMENTS

The authors are indebted to Jan Prokleška for checking the manuscript, providing critical insight and constructive suggestions. This work was supported by the Czech

Science Foundation Grant No. P204/16/06422S and by Charles University, project GA UK No. 720214. Experiments were performed in MLTL (<http://mltl.eu/>) which is supported within the program of Czech Research Infrastructures (Project No. LM2011025).

- 
- \* [michal.valiska@gmail.com](mailto:michal.valiska@gmail.com)
- <sup>1</sup> F. Bloch and G. Gentile, *Zeitschrift für Physik* **70**, 395 (1931).
  - <sup>2</sup> J. H. van Vleck, *Physical Review* **52**, 1178 (1937).
  - <sup>3</sup> J. F. Herbst, *Reviews of Modern Physics* **63**, 819 (1991).
  - <sup>4</sup> M. D. Kuz'min and A. M. Tishin, "Chapter three theory of crystal-field effects in 3d-4f intermetallic compounds," in *Handbook of Magnetic Materials*, Vol. Volume 17, edited by K. H. J. Buschow (Elsevier, 2007) pp. 149–233.
  - <sup>5</sup> D. D. Koelling, B. D. Dunlap, and G. W. Crabtree, *Physical Review B* **31**, 4966 (1985).
  - <sup>6</sup> M. S. S. Brooks and P. J. Kelly, *Physical Review Letters* **51**, 1708 (1983).
  - <sup>7</sup> V. Sechovský, Z. Smetana, G. Hilscher, E. Gratz, and H. Sassik, *Physica B+C* **102**, 277 (1980).
  - <sup>8</sup> J. M. Fournier, A. Boeuf, P. Frings, M. Bonnet, J. v. Boucherle, A. Delapalme, and A. Menovsky, *Journal of the Less Common Metals* **121**, 249 (1986).
  - <sup>9</sup> L. Severin, L. Nordström, M. S. S. Brooks, and B. Johansson, *Physical Review B* **44**, 9392 (1991).
  - <sup>10</sup> P. H. Frings, J. J. M. Franse, A. Menovsky, S. Zemirli, and B. Barbara, *Journal of Magnetism and Magnetic Materials* **54**, 541 (1986).
  - <sup>11</sup> V. Sechovský and L. Havela, "Chapter 1 magnetism of ternary intermetallic compounds of uranium," in *Handbook of Magnetic Materials*, Vol. Volume 11 (Elsevier, 1998) pp. 1–289.
  - <sup>12</sup> G. Busch and O. Vogt, *Journal of the Less Common Metals* **62**, 335 (1978).
  - <sup>13</sup> C. F. Buhner, *Journal of Physics and Chemistry of Solids* **30**, 1273 (1969).
  - <sup>14</sup> J. L. Smith and E. A. Kmetko, *Journal of the Less Common Metals* **90**, 83 (1983).
  - <sup>15</sup> O. Eriksson, M. S. S. Brooks, B. Johansson, R. C. Albers, and A. M. Boring, *Journal of Applied Physics* **69**, 5897 (1991).
  - <sup>16</sup> V. Sechovský, L. Havela, H. Nakotte, F. R. de Boer, and E. Brück, *Journal of Alloys and Compounds* **207-208**, 221 (1994).
  - <sup>17</sup> B. R. Cooper, R. Siemann, D. Yang, P. Thayamballi, and A. Banerjee, *Hybridization-induced anisotropy in cerium and actinide systems* (North-Holland, Netherlands, 1985).
  - <sup>18</sup> B. R. Cooper, G. J. Hu, N. Kioussis, and J. M. Wills, *Journal of Magnetism and Magnetic Materials* **63**, 121 (1987).
  - <sup>19</sup> A. A. Menovsky, *Journal of Magnetism and Magnetic Materials* **76-77**, 631 (1988).
  - <sup>20</sup> H. Rietveld, *Journal of Applied Crystallography* **2**, 65 (1969).
  - <sup>21</sup> J. Rodriguez-Carvajal, *Physica B: Condensed Matter* **192**, 55 (1993).
  - <sup>22</sup> T. Roisnel and J. Rodriguez-Carvajal, in *EPDIC 7 - Seventh European Powder Diffraction Conference*, edited by R. Delhez and E. Mittemeijer (Trans Tech Publications).
  - <sup>23</sup> M. Rotter, H. Müller, E. Gratz, M. Doerr, and M. Loewenhaupt, *Review of Scientific Instruments* **69**, 2742 (1998).
  - <sup>24</sup> B. Lloret, B. Buffat, B. Chevalier, and J. Etourneau, *Journal of Magnetism and Magnetic Materials* **67**, 232 (1987).
  - <sup>25</sup> S. A. M. Mentink, G. J. Nieuwenhuys, A. A. Menovsky, and J. A. Mydosh, *Journal of Applied Physics* **69**, 5484 (1991).
  - <sup>26</sup> E. Du Trémolet de Lacheisserie, D. Gignoux, and M. Schlenker, *Magnetism* (Springer, 2005).
  - <sup>27</sup> K. Koepernik and H. Eschrig, *Physical Review B* **59**, 1743 (1999).
  - <sup>28</sup> A. Arrott, *Physical Review* **108**, 1394 (1957).
  - <sup>29</sup> A. Arrott and J. E. Noakes, *Physical Review Letters* **19**, 786 (1967).
  - <sup>30</sup> B. Widom, *J. Chem. Phys.* **43**, 3892 (1965).
  - <sup>31</sup> P. Weiss, *J. Phys. Theor. Appl.* **6**, 661 (1907).
  - <sup>32</sup> H. Yamada, *Physics Letters A* **55**, 235 (1975).
  - <sup>33</sup> A. V. Andreev, "Chapter 2 thermal expansion anomalies and spontaneous magnetostriction in rare-earth intermetallics with cobalt and iron," in *Handbook of Magnetic Materials*, Vol. Volume 8 (Elsevier, 1995) pp. 59–187.
  - <sup>34</sup> E. R. Callen and H. B. Callen, *Physical Review* **129**, 578 (1963).
  - <sup>35</sup> P. Durga, K. P. Arjun, V. K. Pecharsky, and J. K. A. Gschneidner, *Journal of Physics: Condensed Matter* **25**, 396002 (2013).
  - <sup>36</sup> S. F. Matar, B. Chevalier, and R. Pöttgen, *Solid State Sciences* **27**, 5 (2014).
  - <sup>37</sup> M. Shimizu, *Physica B: Condensed Matter* **159**, 26 (1989).
  - <sup>38</sup> P. Mohn, K. Schwarz, and D. Wagner, *Physica B: Condensed Matter* **161**, 153 (1990).